NON-DESTRUCTIVE EVALUATION OF COMPOSITES MATERIALS BY PULSED-PHASE THERMOGRAPHY: DEPTH INVERSION

Fernando López Rodríguez, flopez@cwpanama.net
Vicente de Paulo Nicolau, vicente@emc.ufsc.br
Hugo Oshiro, oshiro.hugo@gmail.com
Daniel Tancredi, dtancredi@gmail.com

Federal University of Santa Catarina, Mechanical Engineering Department, Florianopolis, Brazil.

Abstract. *This work is focused in the application of Pulsed-Phase Thermography (PPT) to non-destructive evaluation of composite materials. In this approach, the composite sample is heated by a thermal pulse briefly and recording the surface temperature decay with an infrared camera. Data processing and depth inversion is carried out by extracting and analyzing the response of the sample on the frequency domain, based on the frequency spectrum available in the thermal stimulation pulse. The extraction of the various frequencies is performed with a discrete one-dimensional Fourier Transform on each pixel of the thermogram sequence. The depth inversion technique relies on the thermal diffusion length equation in a similar manner as in Lock-In Thermography. Thus, the inversion problem reduces to the estimation of the blind frequency, i.e. the limiting frequency at which a defect at a particular depth presents enough phase contrast to be detected on the frequency spectra. As it will be showed, one of the interesting aspects of PPT is the phase image, which is relatively independent of local optical (e.g. non-uniform heating) and infrared surface features (e.g. variability in surface emissivity). This represents important advances when compared with other techniques, such as Pulsed Thermography.*

Keywords*: infrared thermography, thermal non-destructive test, heat transfer*

1. INTRODUCTION

Non-Destructive Tests (NDT) are methods classified as evaluation techniques for determining the presence of internal irregularities in materials without affect its physical integrity and subsequent service. Within the different NDT methods employed nowadays, Infrared Thermography (IRT) stands as one of the more promissory techniques for the inspection of materials and structures using the principle that all the bodies with temperature above *0 K* emit infrared radiation. Through the measurement of this emitted radiation, IRT allows the detection and characterization of internal defects by analyzing alterations or contrasts in the surface thermal pattern (Maldague, 2001).

IRT as NDT can be deployed using two scheme: passive and active thermography. Passive thermography is basically based on qualitative analysis where no external stimulation is used to provoke thermal gradients on the inspected surface. On the other hand, active thermography requires the induction of an external stimulation in order to produce an internal heat flux within the material. Subsurface defects will affect the heat diffusion rate, producing then a thermal contrast on the surface being test (Rodríguez et al., 2009). Currently, various modes of external stimulation are available, i.e., thermal (Pulsed Thermography, Lock-in Thermography, Long Pulse Thermography, etc.), electromagnetic (Eddy Current Induction) and mechanical (Vibrothermography) excitations are the most widely used. This work is focused in the thermal stimulation techniques.

Among the different thermal excitation methods employed in IRT, Pulsed-Phase Thermography (PPT) (Maldague and Marinetti, 1996) is one of the newest and more attractive processing techniques which combines interesting capabilities of two older approaches: Pulsed Thermography (PT) and Lock-in Thermography (LT). In PT, the acquisition is fast and simple, but defect characterization (or *depth inversion*) is complex, mainly due to the needs of selection a sound area. On the contrary, in LT, acquisition is performed in stationary regime and requires a large number of tests at different modular frequencies (one for every inspected depth); however, the depth inversion procedure is straightforward (Meola and Carlomagno, 2004). As will be showed later in details, acquisition in PPT is performed as in PT and amplitude and phase delay data can be reconstructed as in LT, after applying Fourier Transform on the thermal images collected. Two important aspects stand out when used PPT: contrary to LT, several frequencies are available in a single test and the reliability of using phase images which are less affected by the reflections from the environment, emissivity variations and non-uniform heating.

The depth inversion procedure in PPT still constitutes a wide area of study. Although several studies have proposed interesting inversion procedures using PPT (i.e., statistical method (Vallerand and Maldague, 2000), Neural Networks (Maldague and Couturier, 1998) or PPT Variation Wavelet Transform (Galmiche and Maldague, 2000), none of these approaches were able to provide a practical quantitative inspection technique due to the required calibration steps and lengthy computations (Ibarra-Castanedo, 2005). A new inversion technique, based on phase delay data, has been recently proposed by Castanedo and Maldague (2004a). Quantification is carried out by correlating the defect depth with its corresponding blind frequency, f_b, i.e. the frequency at which the defect becomes visible on the frequency spectra. However, one of the sensitive tasks is the estimation of such *blind frequency* which needs the calculations of phase contrast (or phase delay). As will be shown, the accuracy of this inversion method requires properly selection of acquisitions parameters, such as the time frame rate and truncation window size.

Several works have successfully reported the application of PPT to the NDE of various types of materials, such as steel (Avdelidis et al, 2005), aluminum (Ibarra-Castanedo and Maldague, 2004b) and plexigas (Montani, 2010). However, the extension of this technique to other materials, especially those with high anisotropy, continues been the subject of important studies. In that direction, this work focuses in the NDE of composites materials by PPT. A reference specimen made up of fiberglass and epoxy was used for the thermal tests. Experimental and theoretical aspects of subsurface defect characterization are detailed, concentrating on heat transfer process and thermal wave generation. The potential and limitations of this technique as a reliable depth characterization technique are discussed and futures work will be proposed based on this experience.

2. FUNDAMENTALS OF PULSED PHASE THERMOGRAPHY

Pulsed phase thermography (PPT) can be considered as the link between Pulsed and Lockin Thermography given that combines interesting features from both techniques **(**Maldague et al, 2002**)**. For this reason, next section is dedicated to review the principles of such stimulation and data processing approaches.

2.1. Review of Pulse Thermography and Lock-in Thermography

Pulsed Thermography (PT) is a popular thermal stimulation method in infrared thermography (IRT) whose protocol consists of pulse heating the specimen (being the duration of the pulse applied variable from µs, ms, to s depending on the thickness of the material and its thermal properties, especially the thermal conductivity) and record the temperature decay with an infrared camera. Abnormal behavior of this temperature decay curve reveals subsurface defects. Basically, the phenomenon is as follows: the temperature of the material changes rapidly after the initial thermal perturbation because the thermal front propagates by diffusion; the presence of defects alters (reducing or increasing) the heat diffusion rate so that, when observing the surface temperature, defects appear as areas of different temperatures with respect to a surrounding sound area once the thermal front has reached them **(**Maldague, 2001**)**. The depth inversion is generally based on the computation of the thermal contrast C, which is defined as the temperature difference between the defective and a sane area. Then, for quantitative analysis is of interest the calculation of C_{max} (computed at t_{max}).

In Lock-in-thermography (LT), the specimen's surface is submitted to sinusoidal temperature stimulation while remotely recorded the resulting oscillating temperature field in the stationary regime through its thermal infrared emission with an IR camera. In the stationary regime, the specimen thermal response to such stimulation is also described by a sinusoidal regime whose magnitude and phase depend on the input frequency. In fact, in these conditions, a highly attenuated and dispersive wave sometimes referred to as *thermal wave* stands inside the material. The depth inversion procedure relies in the calculation of the blind frequency (the limiting frequency at which the defect presents enough phase contrast to be detected on the frequency spectra), which can be obtained through the reconstruction on the available frequency spectra of the resulting thermal oscillating wave.

2.2. Principles of Pulsed Phase Thermography

As already mentioned, PPT can be though as being the link between PT and LT. On one hand, PT uses a thermal pulse to stimulate the material and the surface's temperature evolution is recorded in transient regime with an IR camera. Experiments carried out under this configuration are straightforward. On the other hand, LT requires specialized equipment (sinusoidal heating source and lock-in amplifier), but depth quantification is straightforward through the determination of the blind frequency as discussed in Section 2.1.

Although not evident at first sight, a link between PT and LT can be established through the superposition principle. It's well known that any wave, periodic or not, can be approximated by the sum of purely harmonic waves oscillating at different frequencies. Using this concept it is possible to extract thermal waves oscillating at different frequencies from the response of the material after the application of a thermal pulse. Figure 1 illustrates this idea.

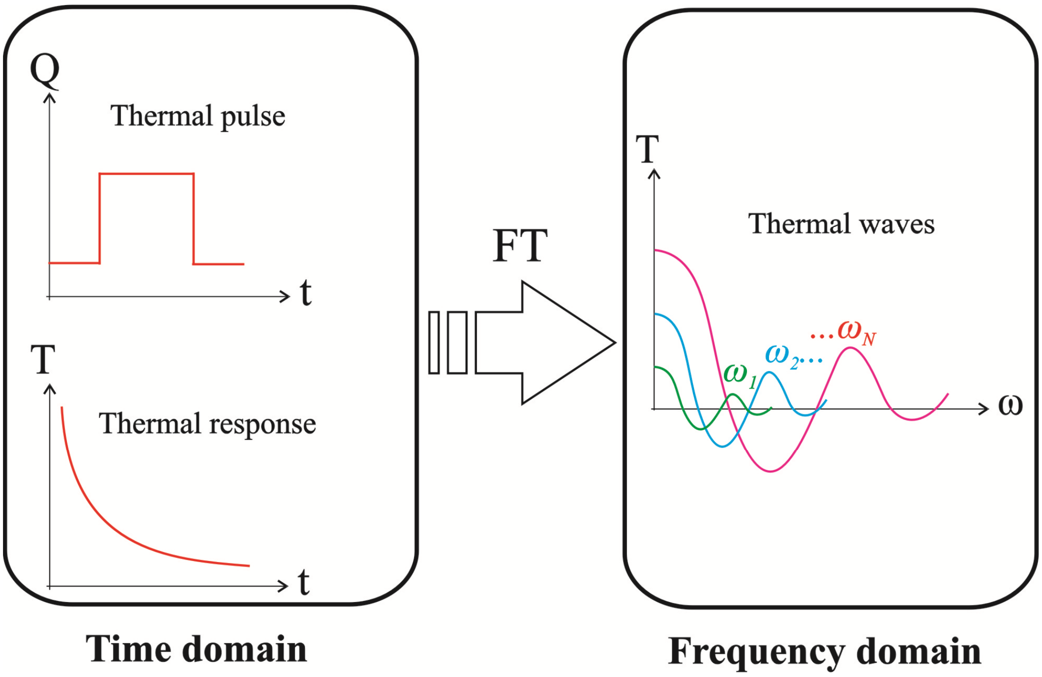

Figure 1. Physical principles of the generation of thermal waves: temporal analysis and its corresponding frequency spectra

On the left side of Fig. 1 is showed the form of the thermal pulse applied to the material by radiation followed by the thermal response of a singular area. It's important to note the time dependence of both: the applied thermal pulse and the surface's thermal response. On the right side are showed thermal waves with different frequency extracted from the thermal response. Hence, PPT goes from the time domain (as in PT) to the frequency domain (as in LT) thanks to the pixel by pixel one-dimensional discrete Fourier Transform (FT) of the thermal sequence:

$$F_n = \Delta t \sum_{k=0}^{N-1} T(k\Delta t) e^{-j2\pi nk/N} = \mathrm{Re}_n + \mathrm{Im}_n \tag{1}$$

In Eq. (1), *T(k)* designates the temperature at location *p* in the k^{th} image of the sequence, *Re* and *Im* are respectively the real and imaginary parts of the transform, the subscript *n* designates the frequency increment ($n=0,1\ldots N$) and Δt is the sampling interval. The sampling interval Δt, is introduced in Eq. (1) as a scale factor in order to produce equivalence between the continuous and discrete Fourier Transform **(**Brighman, 1974**)**. For NDT applications, Eq. (1) is not practical due to length computations. The Fast Fourier Transform (FFT) algorithm, available on software packages such as MatLab®, greatly reduces the computation timing and is therefore privileged. Real and imaginary parts of Eq. (1) are used to calculate the amplitude and the phase of the transform:

$$A_n = \sqrt{\mathrm{Re}_n{}^2 + \mathrm{Im}_n{}^2} \tag{2}$$

and

$$\phi_n = a\tan\left(\frac{\mathrm{Im}_n}{\mathrm{Re}_n}\right) \tag{3}$$

In order to performs the FT on thermal data, the continuous temperature signal *T(t)*, is sampled at Δt intervals (which also depends on IRT systems) and truncated with a rectangular window *w(t)*. Both *w*(*t*) and Δt, or using its reciprocate the sample frequency: $f_s=1/\Delta t$, are strongly dependent on the thermal properties of the material being inspected (Marineti et al., 1999**)**. The sampling theorem ($f_s \geq 2f_c$) should be respected for all defects present on the inspected specimen; the difficulty arises when trying to determine f_c. As a consequence, f_s is generally established empirically by taking some guidelines, e.g. high conductivity materials require a higher f_s to avoid loss of information **(**Ibarra-Castanedo and Maldague, 2004**)**. As for the truncation window *w(t)*, time-duality plays an important role for its determination. Frequency resolution Δf, is directly linked to $w(t)$ through the relationship $\Delta f=1/w(t)$. Several works (for instance Marinetti et al., (1999) and Ibarra-Castanedo et al., (2004)) report advance in the appropriate selection of those two parameters in order to properly characterize defect's depth.

2.3. Data acquisition and processing in PPT

Figure 2 illustrates the main steps in the application of the PPT in NDT and the subsequence routines in the acquisition and data processing. The specimen surface is first stimulated by a thermal pulse coming from halogen lamps. As mentioned, this thermal pulse can vary from microseconds to seconds, depending on the thermophysical properties of the material and defects. Also, PPT can be applied using two different modes: transmission and reflection. In the transmission mode the heat flux is applied by radiation over the surface of the material, so the infrared radiation received by the IR camera is a function of the amount of heat that is transferred by conduction from one side of the material to another. In the reflection mode, the heat front produced by the thermal stimulation propagates through the material until it reaches zones with different thermal properties (or defective zones), reflecting back part of the thermal energy applied. In this work the two modes of application are used in order to determine the best response as possible.

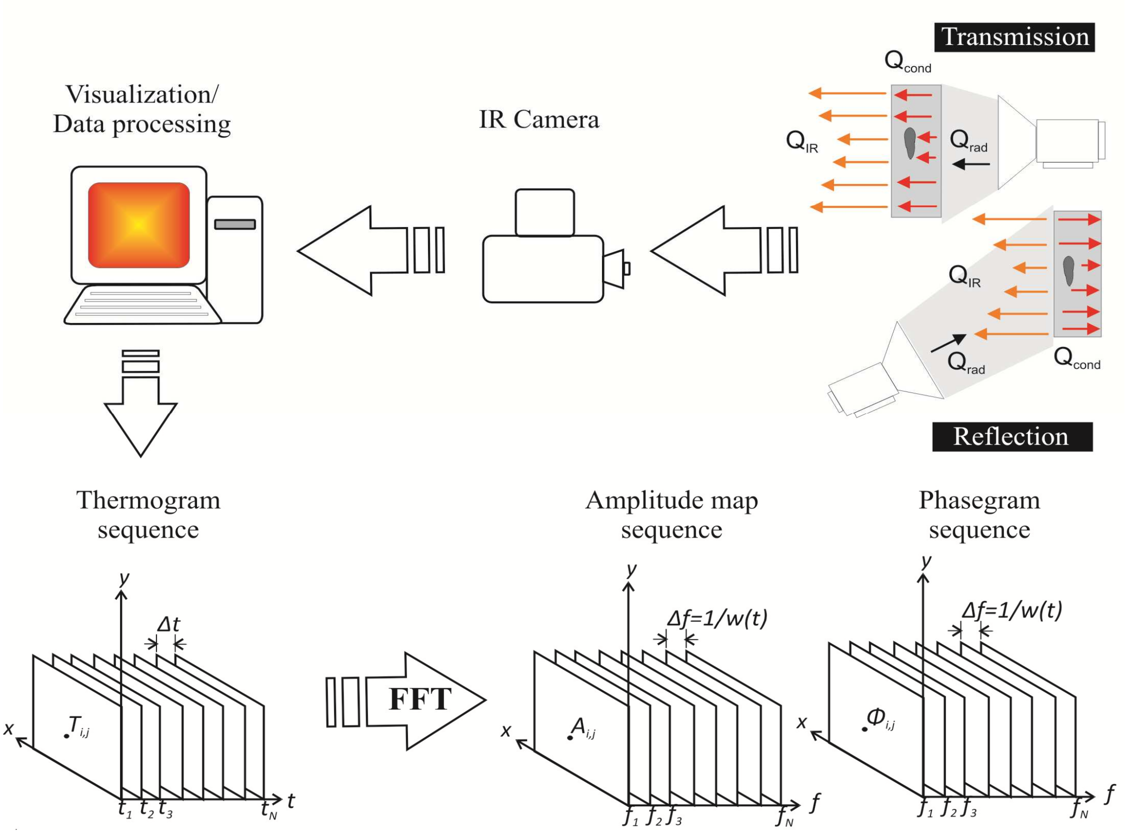

Figure 2. Routines in NDT by PPT

Once the material under inspection is thermally stimulated, the temperature evolution on the surface is monitored using an infrared camera. A thermal map of the surface (or thermogram sequence) is collected at a regular time intervals Δt, forming then a 3D matrix. As showed in Fig. 2, the spatial coordinates (x, y) are represented by the horizontal and vertical pixels positions respectively, whereas z represents the evolution time. The thermogram sequence is then processed applying the Fourier Transform on each pixel of the thermogram sequence by using Eq. (1). Real and imaginary parts of Eq. (1) are used to calculate the amplitude and phase of the transform allowing the reconstruction of the amplitude map and phasegram sequences matrixes, as showed in Fig. (2).

Important features come out when working with frequency data. One of them is that from a sequence of N thermograms, there are $N/2$ useful components; the other half of the spectra only provides redundant information because represents negative frequency data. Another important gain is concerned to the phase response of non-uniform heating. It's well known that phase is practically unaltered by such problems, as well as surface emissivity variations and the presence of non-planar surfaces that typically affect thermal signals. Therefore, there is a great interest in taking advantages of these characteristics for quantitative calculations. In next section is discussed depth inversion procedure using phase data.

2.4. Depth inversion by PPT

The inversion technique used in this work is based on phase delay data which has been proposed by Ibarra-Castanedo and Maldague (2004b). However, before continue with depth characterization procedure, important concepts concerning to thermal waves are explained next.

It's well known from thermal wave's theory that after heating a surface, attenuated and dispersive waves are found inside the material close the surface region. Thus, for a semi-infinite specimen (planar specimen) onto which a uniform source deposits periodically heat with a modulation frequency ω, the mathematical model can be reduced to a one-dimensional problem being the resulting temperature T as a function of depth z and time t due to this periodically stimulation, given by:

$$T(xz,t) = T_o e^{-z/\mu} \cos\left(\frac{2z\pi}{\lambda} - \omega t\right) \tag{4}$$

where μ is the thermal diffusion length expressed by:

$$\mu = \sqrt{2k/\omega\rho c_p} = \sqrt{2\alpha/\omega} \tag{5}$$

with thermal conductivity k, density ρ, specific heat c_p, modulation frequency ω in rad/s, thermal diffusivity α and thermal wavelength λ defined as $\lambda = 2\pi\mu$. From last part of Eq. (4), we also have the phase ϕ of the thermal wave which is directly related to depth z:

$$\phi(z) = \frac{2z\pi}{\lambda} = \frac{z}{\mu} \tag{6}$$

As can be shown in Eq. (6), there will be modulation frequencies for which defects won't be visible. In fact (as in ultrasonic) high frequency thermal waves propagate close to the surface and inversely, low frequency thermal waves propagate deeper. The inversion method proposed by Ibarra-Castanedo and Maldague relies in identifying the so called *blind frequency* f_b, defined as the frequency for which a defect at a given depth can be devised. From Eq. (6) and introducing the phase delay function (defined by $\Delta\phi = \phi_d - \phi_{sa}$), the depth z of defects can be calculated by:

$$z = C\sqrt{\frac{\alpha_{sa}}{f_b\pi}} \tag{7}$$

In Eq. (7), α_{sa} is the thermal diffusivity of the sound area, while C is a correction factor which can taken $C=1$ when working with amplitude data, while for the phase $1.5< C <2$, with $C=1.8$ frequently adopted. Figure (3) shows the phase and phase delay profiles for the case of tick defects (flat-bottomed holes) at two different depths. The phase profiles for the positive part of the spectra for two defects depths (ϕ_{z1}, ϕ_{z2}), and for a sound area (ϕ_{sa}), are shown at the bottom part of this graph. Phase delay can be calculated using the phase delay function previously mentioned.

As seem in Fig. (3), the blind frequency f_b needed to calculate the depth using Eq. (7) corresponds to the point where phase delay reaches zero ($\Delta\phi = \phi_d - \phi_{sa} \approx 0$). Given that (amplitude and) phase information is available in PPT, inversion procedures should be possible through Eq. (7), after determining f_b., as is done by LT; with the advantage that in PPT, several frequencies are available at once, and hence, complete phase profiles can be reconstructed in a single test. Nevertheless, as discussed in Section 2.2, additional difficulties arise in PPT when trying to adequately establish the temporal parameters that will produce the appropriate frequency response. Currently, different studies are conducted in this direction at the laboratory in order reconstruct properly the phase profiles and enhance this inversion technique.

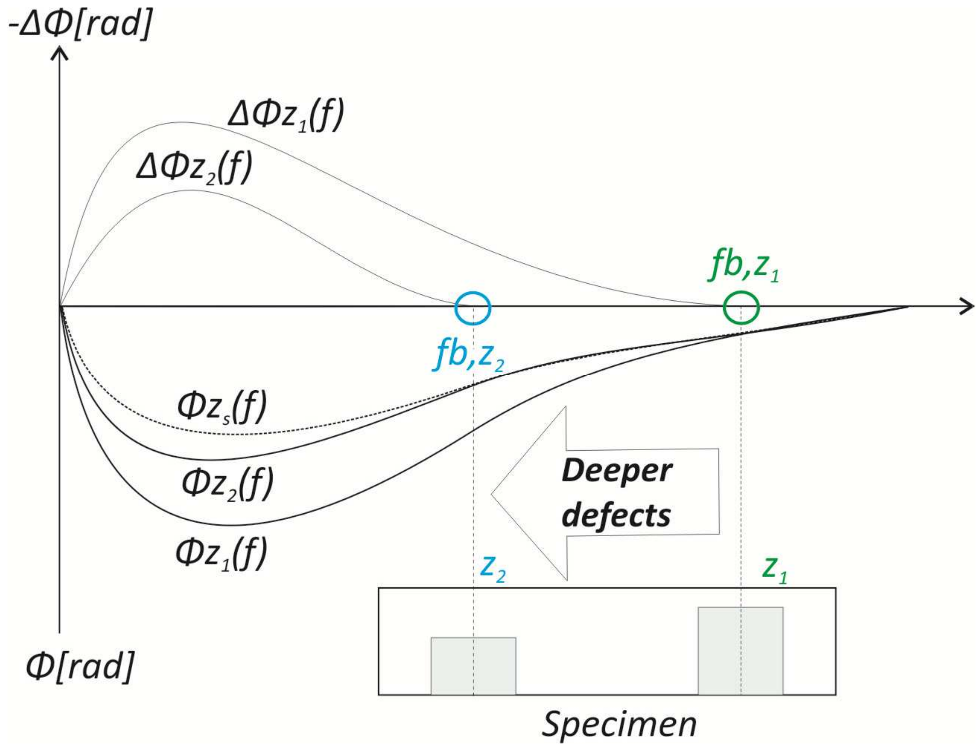

Figure 3.Depth inversion with the phase contrast and blind frequency (modified from Castanedo-Ibarra, 2005)

3. EXPERIMENTAL APPROACH FOR NDE OF COMPOSITES MATERIALS BY PPT

Quantitative analyses by PPT were performed in the specimen showed in Fig. 4. The specimen is a composite material (60 % fiberglass and 40 % epoxy) and presents six (6) flat-bottomed hole defects with depths varying from 0.6 to 2.1 mm. The defects were made of EVA (ethylene-vinyl acetate) and have square shape (30 mm x 30 mm).

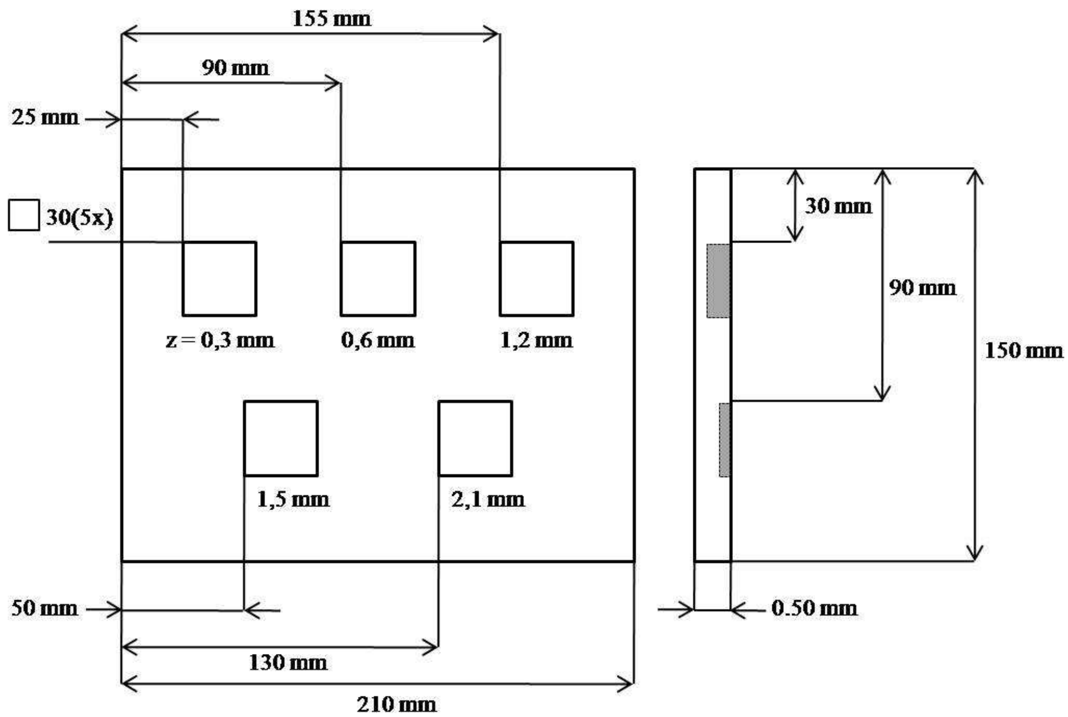

Figure 4. COMP1 Reference specimen studied with flat bottomed hole defects of different depths.

The experimental procedure is the same as showed in Fig. (2). The specimen was first heated with a halogen lamp of 1000 W with pulse durations of 10 and 15 s. The temperature evolution field was monitored using a FPA infrared camera (ThermaCam SC500), on a 320 x 240 pixel array with 14-bit resolution. The infrared data was later analyzed with a Laptop (Corel 2 Duo, 2 GB RAM) using Matlab® language from the MathWorks, Inc.

Different experiments were carried out in order to determine the best deployment and parameters set. As for the deployment, were used the two mode of application: transmission and reflection schemes. Results are showed in next section. The acquisition parameters were studied for the purpose of analyzes their impact in the depth inversion procedure. As mentioned, the range of frequency spam from *0* to $1/\Delta t$ (i.e., the frame rate), where Δt is the time interval between the images in the recorded sequence, while the frequency resolution is given by $\Delta f=1/w(t)= N.\Delta t$, being $w(t)$ the truncation window and N the number of thermal images in the sequence. The maximum frequency available is thus limited by the frame rate resolution, while de frequency resolution is limited by the duration of the experiment.

4. RESULTS AND DISCUSSIONS

The first parameter studied was the difference in the thermal pattern of the surface due to the application mode of the external stimulation. Figures (5) shows the results observing that when used the reflection mode (Fig. 5a), defectives zones present higher temperature than the sane areas. This is a consequence of the resistive effect of the defects that alter the heat flux applied on the surface, causing an increase in temperature due to the accumulation of heat on that region of the material. On the contrary, when using the transmission mode (Fig. 5b), the defectives areas have a lower temperature than its surrounding or sane areas. Using these heat transfer considerations important key-features of the defects can be obtained and to determine what kind of defects are present in the material.

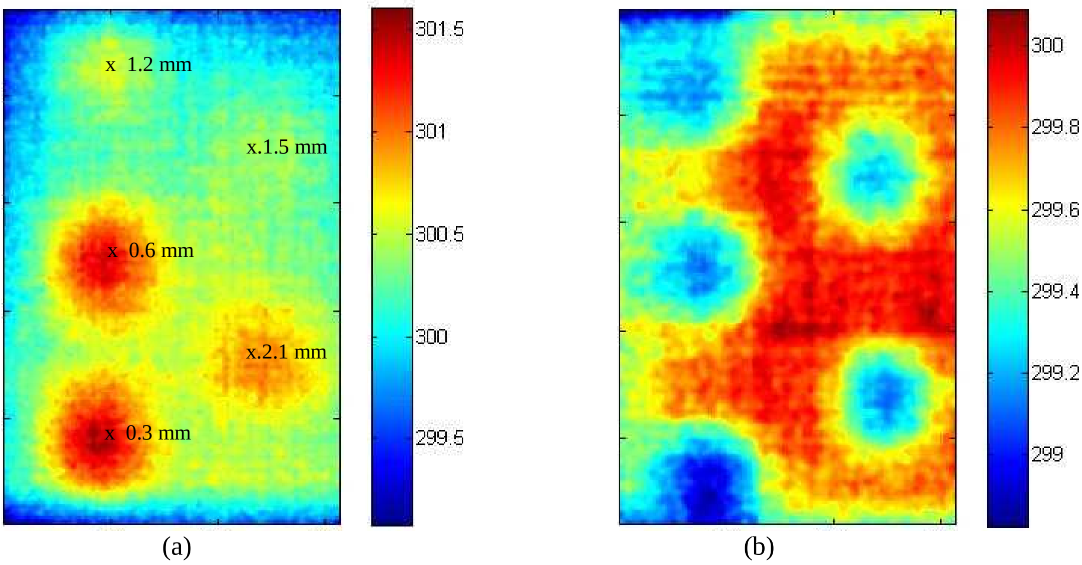

Figure 5. Thermal IR images corresponding to 47 s after the application of a thermal pulse of 1000 W during 5 s, using (a) reflection mode and (b) transmission mode

Figure (6) shows the results of two IR images corresponding to 14 s (Fig. 6a) and 36 s (Fig. 6b) after the application of a thermal pulse of 1000 W and 10 s duration. Acquisition parameters adopted for those results were: $\Delta t = 1$ *frame/s*, $N = 133$ and $w(t) = 133$ *s*. Those parameters were also used after the application of the Fourier Transform to the thermogram sequence collected during the experiments. IrView was used to get the 3D view of the surface temperature distribution and enhance the visibility of the defects. At first observation, it is important to note from those IR images that shallower defects present more thermal contrast than the deeper defects. Also, deeper defects need more observation time to be detected. The defect located and 2.1 mm depth can only be detectable after 36 s, being its thermal contrast very weak.

Figures 7 shows the phasegram (Fig. 7a) and amplitude map (Fig. 7b) at $f = 1$ *Hz* after the application of the Fourier Transform to the thermogram sequence collected. Also, in Fig. (8a) and (8b) are the phasegram and amplitude map, respectively, at $f = 0.66$ *Hz*. The acquisition parameters were set to $\Delta t = 0.5$ *frame/s*, $N = 150$ and $w(t) = 75$ *s*. It is important to note from those figures that are almost unaffected by the non-uniform heating nor emissivity variations when compared to the thermal data of Fig. (6). Also, deeper defects can be seen clearly using phasemaps. This last fact represents an important gain in terms of the detectability of deeper defects when applied the Fourier Transform to the collected IR thermal images

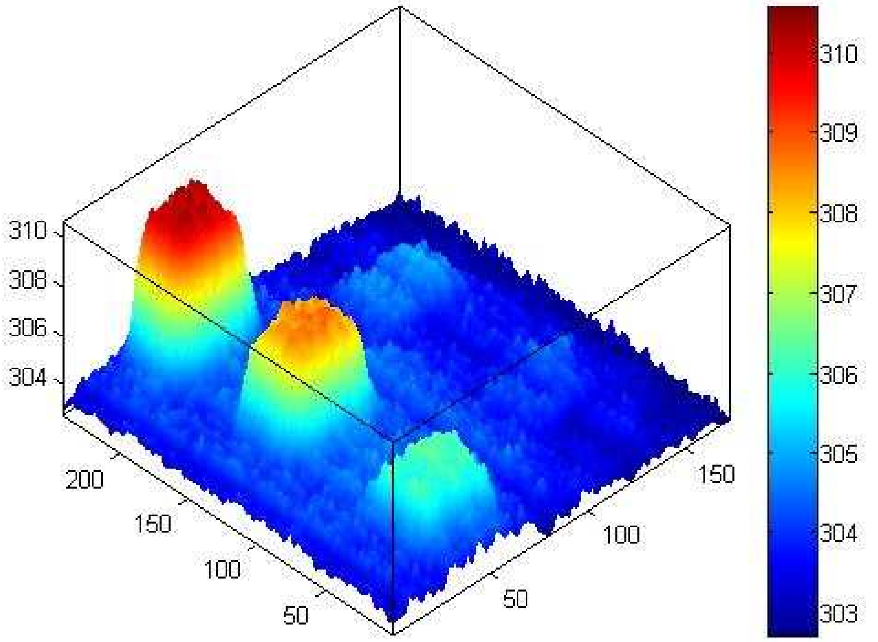

(a)

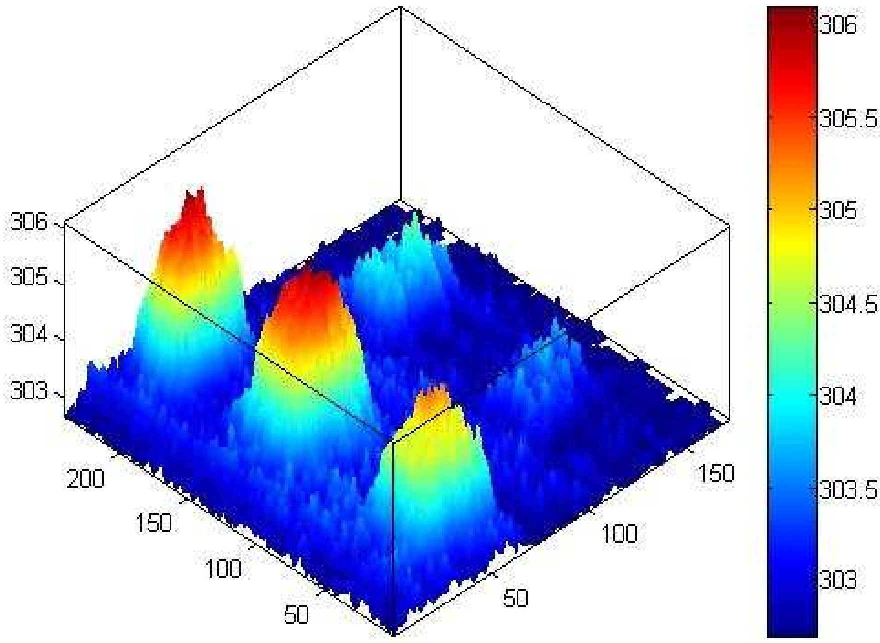

(b)

Figure 6. Thermal IR images corresponding to (a) 14 s and (b) 36 s

Another important point is concerned to the phasegrams, which relate the phase delay of the thermal waves present at every single pixel of the matrix. Is shown in Fig. 7(a) and 8(a) that deeper defects present more phase contrast (or phase delay) at high frequencies, which ratifies the relation by Eq. (7). By the other hand, shallower defects will be clearly visible at higher frequencies.

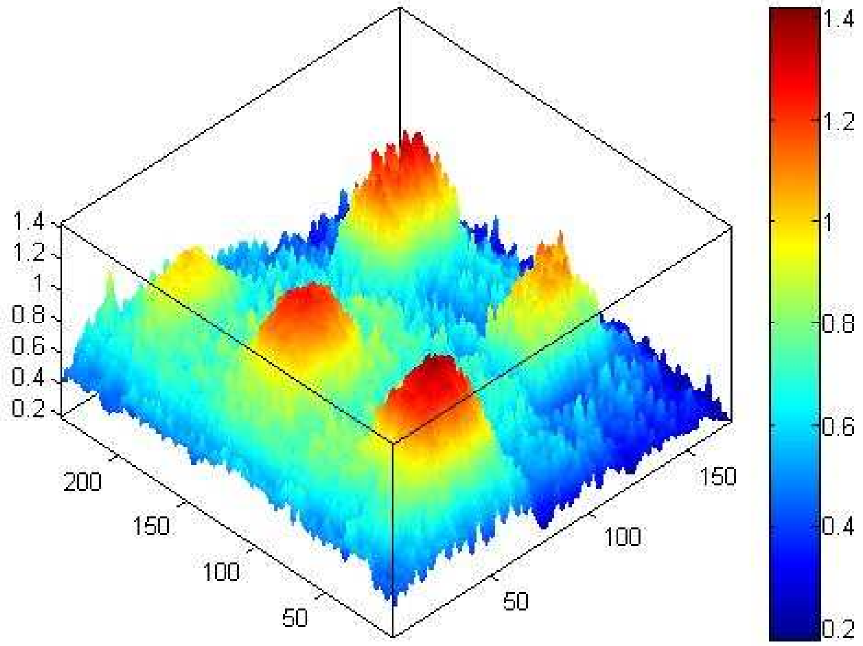

(a)

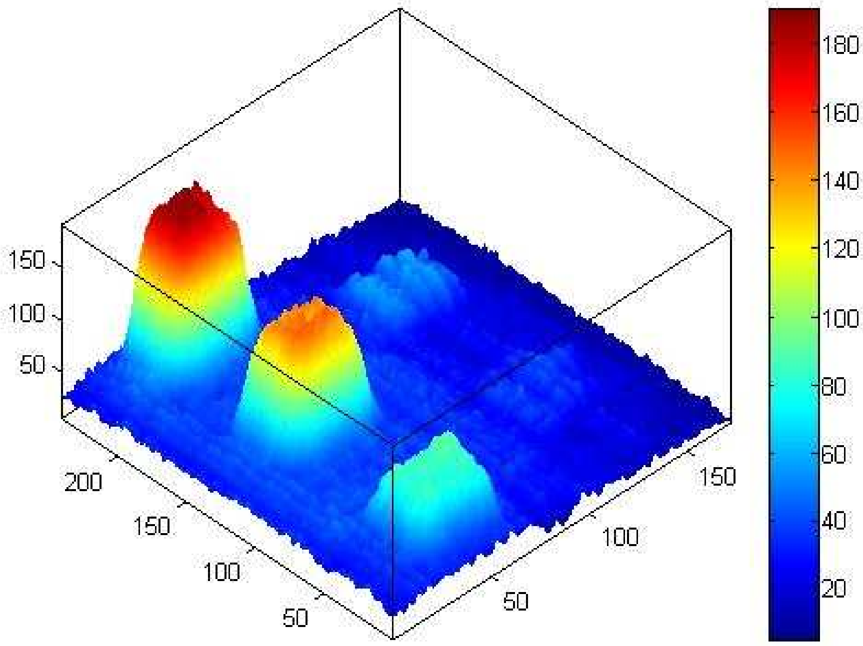

(b)

Figure 7. Phase and amplitude images, both at *f=1 Hz*.

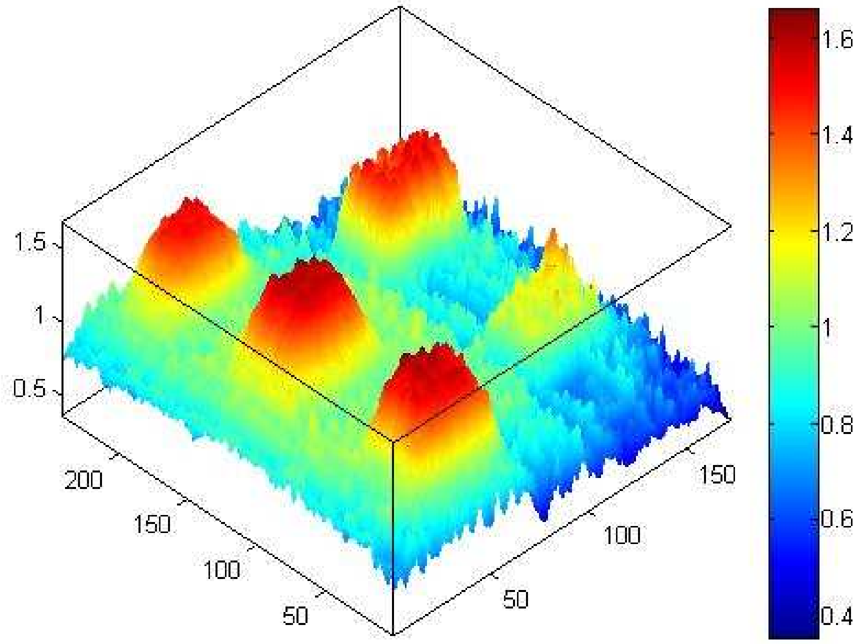

(a)

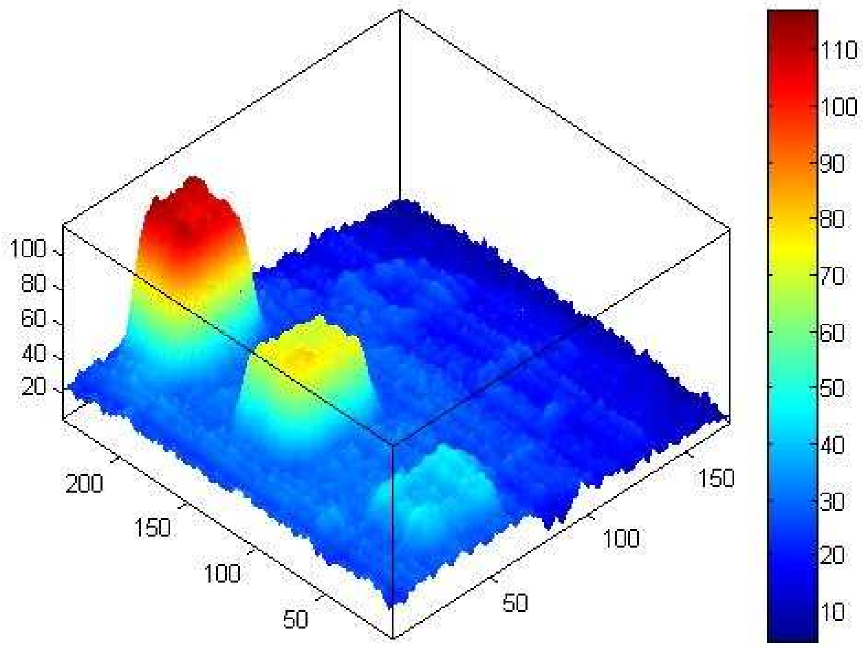

(b)

Figure 8. Phase and amplitude images, both at *f=0.66 Hz*.

Table 1 shows the results of the depth inversion in PPT using the method proposed by Ibarra-Castanedo and Maldague. The optimum set of acquisition parameters resulting the better achieved results were: *Δt = 1 frame/s*, *N = 120* and *w(t) = 120 s*. The duration of the thermal pulse was of 10 s and also the reflection mode was used. The best results were obtained in the estimation of the deeper defects, as is showed in Table (1). Different circumstances affected the accuracy of the inversion method, such as the lack of the real thermophysical properties used in the calculation of the thermal diffusion length. Another important factor is related to the maximum acquisition rate of the infrared camera, which is *1 frame/s*. This means that the maximum frequency available was of *0.83 Hz*, which is quite below what is really needed to properly characterize shallower defects. It's important to remember that the frequency resolution is closely related to such acquisition rate and also represents an important factor that affects the precision of this method.

Table 1. Results of depth inversion by PPT.

Z_{real} (mm)	CI	f_b (Hz)	α_{sa} (mm^2/s)	Z_{PPT} (mm)	Error (%)
2,10	2,26	0,08	2.1 x10^{-7}	2,02	3,61
1,50	2,26	0,14	2.1 x10^{-7}	1,57	-4,52
1,20	2,26	0,17	2.1 x10^{-7}	1,43	-19,27
0,60	2,26	0,42	2.1 x10^{-7}	0,91	-50,87
0,30	2,26	0,83	2.1 x10^{-7}	0,64	-113,36

5. CONCLUSIONS

In this work has been presented the theory and application of Pulsed-Phase Thermography for non-destructive tests in composites materials. As properly proved in this paper, PPT has interesting capabilities in the detection and depth inversion, especially when compared to traditional techniques such Pulsed and Lock-in Thermography. However, PPT presents limitations when analyzing shallower defects: higher frequencies must be available in order to proper retrieve the depth of the defects. As mentioned, this limitation can be compensated with infrared cameras with higher sample frequencies. Further works include the numerical simulation of the heat transfer process during the stimulation and the thermal response of the material when applying different amount of radiation at the surface of the specimen being analyzed, aiming to determine the best conditions for detecting deeper defects.

6. ACKNOWLEDGEMENT

The authors would like to thanks the financial support given by the CNPq. Oshiro received a grant from the "Programa de Recursos Humanos da ANP para o Setor de Petróleo e Gás Natural - PRH09-ANP/MME/MCT"

7. REFERENCES

Avdelidis N.P., Ibarra-Castanedo C. and Maldague X., 2005. "Quantitative Pulsed Phase Thermography Applied to Steel Plates," Proceedings of SPIE – The International Society for Optical Engineering, Thermosense XXVII, pp. 342-351.

Brighman E. O., 1974. "The Fast Fourier Transform," Englewood Cliffs, Prentice-Hall, Inc., NJ.

Clemente Ibarra-Castanedo, 2005. "Quantitative Subsurface defect Evaluation by Pulsed Phase Thermography: Depth Retrieval with the Phase." Ph.D. Thesis, Université Laval.

Rodríguez F. L., Nicolau V. P., Bonin E., 2009. "Infrared thermography applied to ceramic materials: numerical analysis and experimental results," Proc. International Congress of Mechanical Engineering (COBEM), Gramado-Brazil. COB09-2604.

Galmiche F. and Maldague X., 2000. "Depth Defect Retrieval Using the Wavelet Pulsed Phased Thermography," Proc. 5th Conference on Quantitative Infrared Thermography (QIRT), Eurotherm Seminar 64, pp.194-199.

Ibarra-Castanedo C. and Maldague X., 2004a. "Pulsed Phase Thermography Reviewed," Journal of Quantitative Infrared Thermography, Vol. 1, No. 1, pp.47-70

Ibarra-Castanedo C. and Maldague X. 2004a. "Defect Depth Retrieval from Pulsed Phase Thermographic Data on Plexiglas and Aluminum Samples," Thermosense XXVI, Proc. SPIE, Vol. 5405, pp. 348-356.

Ibarra-Castanedo C. and Maldague X., 2004c. "Defect Depth Retrieval from Pulsed Phase Thermography Data on Plexigas and Aluminum Samples," Proceedings of SPIE – The International Society for Optical Engineering, Thermosense XXVI, pp. 348-355.

Maldague X., 2001 "Theory and Practice of Infrared Technology for Nondestructive Testing," John Wiley & Sons, NY.

Maldague X. and Couturier J.P., 1997. "Review of Pulse Phase Infrared Thermography," Proc. 4th International Workshop on Advanced Infrared Technology and Applications (AITA), Firenze, Italy, Vol. 1, No. 53, pp.271-286.

Maldague X. and Marinetti S., 1996. "Pulse Phase Infrared Thermography," Journal of Applied Physics, Vol. 79, No. 5, pp.2694-2698.

Marinetti S., Plotnikov Y. A., Winfree W. P. and Braggiotti A., 1999. "Pulse Phase Thermography for Defect Detection and Visualization," Proc. SPIE, vol. 3586, p. 230-238.

Meola C. and Carlomagno G.M., 2004. "Recent Advances in the Use of Infrared Thermography," Research in Nondestructive Evaluation, Vol. 3, No. 2, pp.101-124.

Montani R., 2010. "Quantitative Determination of Subsurface Defects in a Reference Specimen Made of Plexigas by Means of Lock-in and Pulse Phase Thermography," Infrared Physics and Technology, Vol. 53, pp.363-371.

Vallerand S. and Maldague X., 2000. "Defect Characterization in Pulsed Thermography: A Statistical Method Compared with Kohonen and Perceptron Neural Networks," NDT&E International, Vol. 5, No. 33, pp.307-315.

8. RESPONSIBILITY NOTICE

The authors are the only responsible for the printed material included in this paper.